Vol. 86 (1994) *ACTA PHYSICA POLONICA A* No. 6

EPR APPLICATION IN THE STUDY OF $K_3H(SO_4)_2$ PROTON CONDUCTOR DOPED WITH Mn^{2+} OR VO^{2+} IONS

S. WAPLAK

Institute of Molecular Physics, Polish Academy of Sciences
Smoluchowskiego 17/19, 60-179 Poznań, Poland

(Received July 4, 1994)

The EPR of Mn^{2+}- or VO^{2+}-doped superprotonic conductor $K_3H(SO_4)_2$ is studied in the 80–471 K temperature range. VO^{2+} EPR spectrum reveals diffusion induced merging of proton transferred superhyperfine structure above 380 K. Line width anomaly is observed in Mn^{2+} EPR spectrum which is attributed to the intrabond and interbond proton motions, these lead to high protonic conductivity. It is shown that paramagnetic centers namely of electronic spin greater than 1, with excess charge compensated by the protonic vacancy, are good probes to monitor the protonic conductivity on molecular level.

PACS numbers: 61.50.–f, 76.30.–v

1. Introduction

Tripotasium hydrogen disulfate $K_3H(SO_4)_2$ belongs to the $Me_3H(AO_4)_2$ crystals family (Me = K, NH_4, Cs, Rb; A = S, Se) with the space group $A2/a$ and it exhibits ferroelastic properties below 471 K [1, 2]. The number of protons in these crystals is several times smaller than the number of possible hydrogen bonds. As a result a dynamically disordered network of hydrogen bonds is formed at higher temperatures leading to the high protonic conductivity of the order of $10^{-2}\ \Omega^{-1}\ cm^{-1}$ [3–6].

Since the translational motions (charge transport) represent the slowest dynamical processes in the proton conductors, and the intersite hopping times are usually of the order of 10^{-8} s [7], the X-band EPR of Mn^{2+} or VO^{2+} paramagnetic centers is expected to be a sensitive tool to study proton motions.

Both VO^{2+} or Mn^{2+} ions occupy the K^+ site positions and involve protonic vacancies needed for the charge compensation. Furthermore we expect that the proton/vacancy motions should be reflected in the EPR spectra of paramagnetic probes.

This paper is organized as follows: Sec. 2 gives a brief account of the experimental conditions; Secs. 3 and 4 present the EPR of Mn^{2+} and VO^{2+} spectra description; the EPR line width anomalies of Mn^{2+} spectra are presented in Sec. 5. The results are discussed and conclusions are given in Sec. 6.

2. Experimental

Hexagonal plate-like crystals doped with VO^{2+} or Mn^{2+} ions were grown isothermally at 295 K from saturated aqueous solutions containing 19 wt% K_2SO_4, 12.7 wt% H_2SO_4 and 0.3 wt% $VOSO_4 \cdot 5H_2O$ or $MnSO_4 \cdot 5H_2O$.

Single crystals with ten times higher Mn^{2+} concentration (10c) were also prepared. A differential thermal analysis (DTA) in these crystals reveals three endothermal peaks at 448 K, 471 K and 518 K. Optical inspection of the single crystal in polarized light reveals the ferroelastic domain pattern which vanishes at 471 K. At about 518 K melting of the specimen is observed. EPR measurements were made with X-band spectrometer operating at 9.2 GHz with the system of temperature control (77–500) K and stabilization.

3. EPR of Mn^{2+}

The XYZ orthogonal laboratory frame chosen for EPR line anisotropy pattern is related to a, b, c crystallographic axes [8] as: $\boldsymbol{X} \parallel \boldsymbol{a}$, $\boldsymbol{Y} \parallel \boldsymbol{b}$ and $\boldsymbol{Z} \parallel \boldsymbol{a} \times \boldsymbol{b}$. After performing the EPR anisotropy measurements we have found that the main crystal field gradient V_{zz} component of Mn^{2+} complex makes the angle 35° with X-axis in ZX plane and is tilted by 12° from this plane. V_{zz} axes orientation in the crystal reflects 120° ferroelastic domain structure with the EPR line intensity ratio to be proportional to the volume of the respective domains. The EPR spectrum of Mn^{2+} ion in a single domain consists of 5 fine structure components ($S = 5/2$), each of them split into 6 hyperfine lines due to the nuclear spin ($I = 5/2$) interaction. The EPR fine structure of Mn^{2+} ion can be described by spin Hamiltonian of monoclinic symmetry [9]

$$H = gB\boldsymbol{H} - 2/3b_4(O_4^0 + 20\sqrt{2}O_4^3) + b_2^0O_2^0 + b_2^2O_2^2 + b_4^0O_4^0, \tag{1}$$

where O_n^m — spin operators, b_n^m — crystal field parameters. The following equations for spin-resolved transitions [10] are obtained for $\boldsymbol{V}_{zz} \parallel \boldsymbol{H}$:

$$(\pm 5/2 \Leftrightarrow \pm 3/2); H_{1,5} = H_0 \mp 4D \pm 4/3(a - F) + 4E^2/H_0,$$

$$(\pm 3/2 \Leftrightarrow \pm 1/2); H_{2,4} = H_0 \mp 2D \mp 5/3(a - F) - 5E^2/H_0,$$

$$(+1/2 \Leftrightarrow -1/2); H_3 = B_0 - 8E^2/H_0, \tag{2}$$

where the resonances H_i magnetic fields are taken for the gravity center of each 6 hyperfine components and $H_0 = h\nu/g$, g is the spectroscopic factor, and $a = 120b_4^0$, $D = 3b_2^0$, $F = 180b_4^0$, $E = 3b_2^2$. The crystal field parameters evaluated from Eq. (2) at room temperature are collected in Table, and the hyperfine constant value $A_{\parallel} = 9$ mT.

TABLE

Spin Hamiltonian parameters of Mn^{2+} ion $K_3H(SO_4)_2$ at room temperature.

g	D [mT]	E [mT]	$(a-F)$ [mT]
1.990	61.55	12.01	−1.05

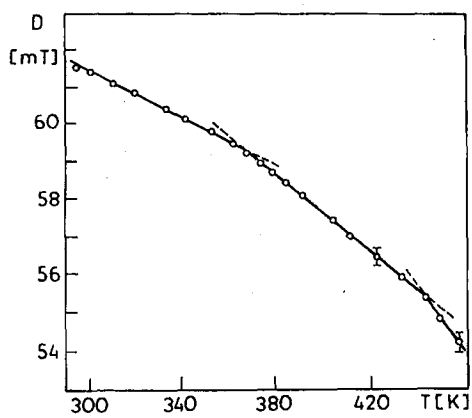

Fig. 1. The temperature dependence of D-axial crystal field parameter of Mn^{2+} EPR spectrum in $K_3H(SO_4)_2$.

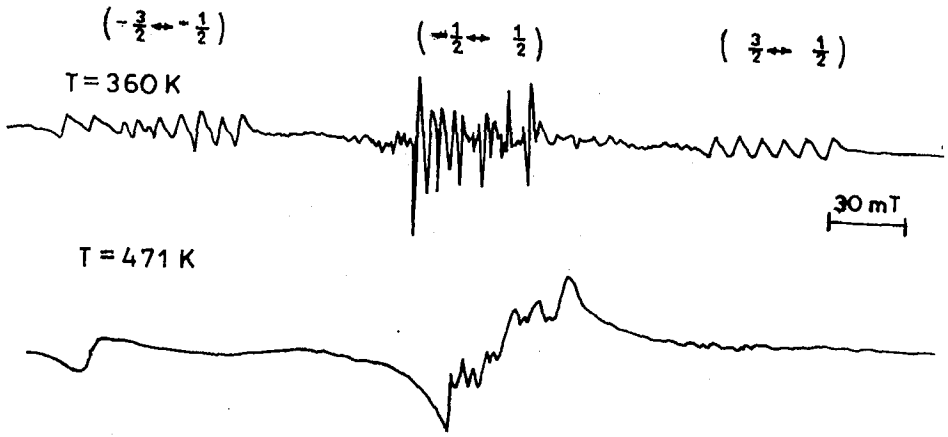

Fig. 2. EPR spectra of Mn^{2+} ion in $K_3H(SO_4)_2$ at 360 K and 471K.

The temperature dependence of the axial crystal field D-parameter in the (300–460) K temperature range is shown in Fig. 1. The specific features of Mn^{2+} spectra in $K_3H(SO_4)_2$ are the broadening and decay of $M \neq 1/2$ fine structure line, reduction of D-value and appearance of the broad line (with $g \cong 2$, $\Delta H_{pp} \cong$

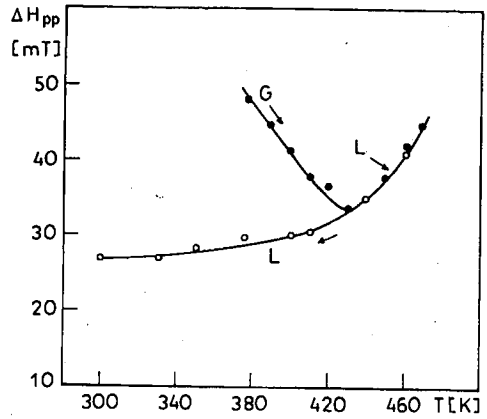

Fig. 3. The broad ($g \cong 2$) Mn^{2+} EPR line width and line shape evolution versus temperature.

50 mT) at about 380 K on the sample heating. The part of the EPR spectrum of Mn^{2+} at 360 K and 471 K is shown in Fig. 2 (the outer lines corresponding to the $\pm 5/2 \Leftrightarrow \pm 3/2$ transitions at 360 K are not shown). The broad line intensity grows up with a temperature increase and the line shape changes from Gaussian to Lorentzian at about 430 K. For the samples heated below 471 K and cooled down, the broad line disappears at about 380 K and simultaneously the amplitudes of the outer $M \neq 1/2$ fine structure lines grow up. In the samples heated to a few degree above 471 K and then cooled down, both EPR lines are present, but now the broad line has the Lorentzian shape. Figure 3 displays the broad line width and line shape anomalies versus temperature for the sample heated up to 473 K.

Before discussing the anomalies observed for Mn^{2+} spectra we will briefly present the similar temperature studies of VO^{2+} ion EPR spectra in $K_3H(SO_4)_2$.

4. EPR of VO^{2+}

The spectrum of VO^{2+} ion ($S = 1/2$, $I = 7/2$) with a hyperfine structure is described by the following spin Hamiltonian parameters: g_{zz}=1.923, g_{xx}=1.979, $g_{yy} = 1.983$; $A_{zz} = 20.27$ mT, $A_{xx} = 7.09$ mT and $A_{yy} = 7.45$ mT. Below 471 K, the individual hyperfine line width varies with temperature in the entirely different manner than that for Mn^{2+} lines. The $\Delta H_{pp}(T)$ of VO^{2+} line width increases linearly with the temperature and $d(\Delta H_{pp})/dT$ slope changes at 380 K.

Direct information on the proton dynamics in $K_3H(SO_4)_2$:VO^{2+} may be learned from the superhyperfine structure (hyperfine structure from ligands) of each hyperfine components due to vanadium nuclear spin interaction with two close equivalent protons leading to the triplets with the intensity ratio 1 : 2 : 1 (Fig. 4).These superhyperfine triplets (shf) are smeared out at about 380 K where protons hopping rate τ becomes comparable with shf structure coupling A^H/h, where h is Planck constant. For proton superhyperfine (shf) value $A^H = 0.75$ mT yields τ of the order of 10^{-11} s.

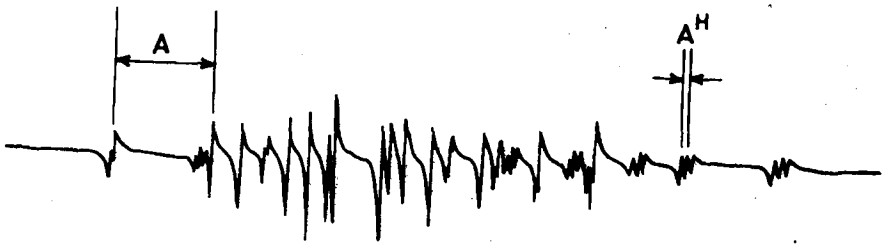

Fig. 4. The hyperfine ($S = 1/2$, $I = 7/2$) and superhyperfine ($S = 1/2$, $I = 7/2$, $I^H = 1/2$) structures of VO^{2+} ion in $K_3H(SO_4)_2$. (A — hyperfine, A^H — superhyperfine constant).

5. Mn^{2+} spectra line width anomalies

As we mentioned above two kinds of ΔH_{pp} anomalies were recorded:

(a) $\Delta H_{pp}(T)$ anomalous changes of hyperfine components of outer $M \neq 1/2$ fine structure lines and lack of anomaly for central $M = 1/2$ line.

(b) The appearance, at about 380 K, of the new broad line with anomaly of the width and shape.

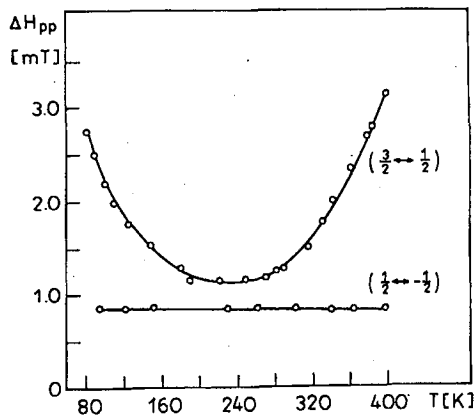

Fig. 5. The hyperfine components of $M = 3/2$ and $M = 1/2$ EPR line width of Mn^{2+} versus temperature (circles = experimental, solid line = fit in accord with Eq. (4)).

Such types of anomalies are unusual for solids, but similar anomalies have been observed for Mn^{2+} spectra in superionic fluorites [11, 14]. Figure 5 presents ΔH_{pp} line width for electronic transitions $M \neq 1/2$ and $M = 1/2$ as a function of temperature. Lack of $\Delta H_{pp}(T)$ changes for $M = 1/2$ line suggests that $M \neq 1/2$ line anomalies are due to the crystal field modulation and the experimental points in Fig. 5 are well fitted by the solid line calculated from the expression

$$\Delta H_{pp}(T) = \Delta H^0_{pp} + (2M - 1)D^2/\omega_0 [(T - T_0)/T_0]^2 , \qquad (4)$$

where D — axial crystal field parameter for a given temperature, ω_0 is EPR

frequency, ΔH_{pp}^{0} is the residual line width separately for $M = 1/2$ or $M \neq 1/2$ fine structure lines at T_0.

In the case (b) the broad line width anomaly looks similar to (a) but their origins have to be different.

Below we discuss the origins of these anomalies.

6. Discussion

The crystal field of predominantly axial symmetry at Mn^{2+} site can be attributed to protonic vacancy and D-value decreasing at higher temperatures is due to the increase in Mn^{2+}-vacancy distance. The Mn^{2+}-vacancy spectrum is extremely sensitive to the crystal field modulation because, the fine structure spectra ($S = 5/2$) as a rule vary as λ^2/Δ, whereas it is linear with λ/Δ, in the case of $S = 1/2$ (Δ is crystal field parameter, λ is spin–orbit coupling constant) [12]. It is the reason why the unusual $\Delta H_{pp}(T)$ of $M \neq 1/2$ line width variations are observed only in Mn^{2+} and they reflect directly the vacancies movements, whereas the VO^{2+} spectra are affected by the protons movements.

To explain the $\Delta H_{pp}(T)$ anomaly (a) of basic Mn^{2+} EPR spectrum (that of fine and hyperfine structure) we have to depend on the results of the earlier NMR studies regarding the proton motions in protonic conductors of KH_2PO_4 (KDP) family [13]. Using NMR, Schmidt et al. [13] have measured the motions of deuterons in KD_2PO_4 crystal. They have distinguished two types of deuteron (proton) motions: interbond and intrabond to be driven by activation processes. They have found that T_1 spin–lattice relaxation time of the intrabond proton motion decrease with a temperature rise while the opposite is observed for the interbond proton motions. The resulting value of $(T^*)^{-1}$ has a minimum at about 285 K for KDP. Assuming that the $\Delta H_{pp}(T)$ width observed in our measurements reflects both types of proton or vacancy movements by the crystal field modulation of Mn^{2+} spectrum, hence the line width anomaly would be $\Delta H_{pp} \sim (T^*)^{-1}$ and $T_0 = 230$ K value is the temperature of $(T^*)^{-1}$ minimum.

Such a mechanism of proton/vacancy dynamics is valid up to 380 K above which the proton diffusion becomes responsible for the occurrence of the broad line. (Note that protons superhyperfine structure of VO^{2+} is averaged out at about 380 K.) This diffusion, up to about 430 K, is of a random type leading to Gaussian line shape. Above 430 K, where the correlation time τ for diffusion is of order of ω_0 (EPR) the line shape tends to be Lorentzian. To distinguish between the vacancy movement and Mn^{2+} ion movement at high temperatures suggested by Minge [2] we compare the broad line behavior for (c) and ($10c$) Mn^{2+} concentrations. The amplitude of the broad line for $10c$ is relatively weaker than for c concentration and the broad line for $10c$ sample occurs at higher temperature. This indicates that autocorrelation function of broad line decay at the vacancy hopping rate ω/c and not the cation hopping rate ω [14] in the transport processes below 471 K. The similar conclusion has been drawn from NMR studies of $CsHSeO_4$ in reference to Cs motion [15].

It is worth noticing here that up to about 380 K the proton/vacancy movements seem to be restricted to the proton jumps inside $(SO_4H \cdot SO_4)^{3-}$ dimers and between nearest-neighboring dimers in $K_3H(SO_4)_2$. Next, above 380 K, pro-

ton diffusion involving the distant dimers is activated. Then the proton transport in $K_3H(SO_4)_2$ occurs through normal and interstitial protonic sites.

We have shown that paramagnetic probes with EPR fine structure spectra ($S > 1/2$) evoked by protonic vacancy are good probes for the study of proton conductors.

References

[1] K. Gesi, *J. Phys. Soc. Jpn.* **48**, 886 (1980).

[2] J. Minge, *Ferroelectrics* **80**, 23 (1980).

[3] Yu.N. Moskvich, A.M. Polykov, A.A. Sukovsky, in: *24-th AMPERE Congress, Magnetic Resonance and Related Phenomena*, Poznań 1988, Eds. J. Stankowski, N. Piślewski, S.K. Hoffmann, S. Idziak, Elsevier, Amsterdam 1989, p. 529.

[4] A.I. Baranov, V.P. Kniznichenko, L.A. Shuvalov, *Ferroelectrics* **100**, 135 (1989).

[5] A.I. Baranov, I.P. Makarova, L.A. Muradyan, V.I. Simonov, A.V. Tregubchenko, L.A. Shuvalov, *Kristallografiya* **32**, 682 (1987).

[6] A.D. Reddy, S.G. Sathyanarayan, G.S. Sastry, *Solid State Comm.* **43**, 937 (1982).

[7] R.C.T. Slade, *Solid State Comm.* **53**, 927 (1985).

[8] Y. Noda, S. Uhiyama, K. Kafuku, H. Kasatani, H. Terauchi, *J. Phys. Soc. Jpn.* **59**, 2804 (1990).

[9] A. Abragam, B. Bleney, *Electron Paramagnetic Resonance of Paramagnetic Ions*, Claredon Press, Oxford 1980.

[10] R. Hrabański, Ph.D. Thesis, Poznań 1980.

[11] C. Evora, V. Jaccarino, *Phys. Rev. Lett.* **39**, 1554 (1977).

[12] G.E. Pake, *Paramagnetic Resonance*, New York 1962.

[13] V.H. Schmidt, E.A. Uehling, *Phys. Rev.* **126**, 447 (1962).

[14] J. Shinar, V. Jaccarino, *Phys. Rev. B* **37**, 4034 (1983).

[15] Yu.N. Moskvitch, A.M. Polykov, A.A. Suchovsky, *Fiz. Tverd. Tela* **30**, 45 (1988).